Modern Physics Letters B
Vol. 31, No. 17 (2017) 1750195 (8 pages)
© World Scientific Publishing Company
DOI: 10.1142/S0217984917501950

Mod. Phys. Lett. B 2017.31. Downloaded from www.worldscientific.com
by UNIVERSITY OF SCIENCE AND TECHNOLOGY OF CHINA on 06/06/18. For personal use only.

Magnetic and electrical transport properties of $Sr_2Ti_{1-x}Co_xO_4$ ceramics by sol–gel

Li Zhang*,‡, Yibao Li*, Zhen Tang*, Yan Deng*, Hui Yuan*, Jiangying Yu* and Xuebin Zhu†

*Department of Mathematics and Physics, Anhui University of Architecture, Hefei 230022, China
†Key Laboratory of Materials Physics, Institute of Solid State Physics, Chinese Academy of Sciences, Hefei 230031, China
‡lizhang@ahjzu.edu.cn

Received 24 February 2017
Revised 9 April 2017
Accepted 17 April 2017
Published 8 June 2017

Microstructures, electrical transport and magnetic properties of $Sr_2Ti_{1-x}Co_xO_4$ ($0 \leq x \leq 0.3$) ceramics are investigated. With Co doping, the $Sr_2Ti_{1-x}Co_xO_4$ ceramics remain tetragonal structure while the grain size is decreased with doping. Magnetic moment is enhanced with Co doping and ferromagnetism is observed at low temperatures for Co-doped Sr_2TiO_4. The $Sr_2Ti_{0.9}Co_{0.1}O_4$ and $Sr_2Ti_{0.7}Co_{0.3}O_4$ show semiconductor-like transport properties, which can be well fitted by Mott variable range hopping model. The results will provide an effective route to synthesize $Sr_2Ti_{1-x}Co_xO_4$ ceramics as well as to investigate the physical properties.

Keywords: Sr_2TiO_4; ceramic; magnetic property; electrical transport property.

1. Introduction

The two-dimensional layered perovskites with chemical formula of A_2BO_4 have attracted broad interests since the discovery of high temperature superconductivity in $La_{2-x}Ba_xCuO_4$.[1–3] In this structure, the perovskite-structured ABO_3 layers are separated by rock salt A–O layers, and the B–O–B interactions can only occur within the *ab* plane.[4] The electronic structures could be systematically studied as the occupation of *d* orbitals increases from empty (d^0 for Ti^{4+}) to half-filled (d^5 for Co^{4+}). In the d^0 case, the Sr_2TiO_4 is always a nonmagnetic insulator.[5] On the other hand, for the d^5 case, it is reported that Sr_2CoO_4 is a ferromagnetic metal with

‡Corresponding author.

ferromagnetic–paramagnetic (FM–PM) transition Curie temperature $T_c \sim 250$ K, and its crystal structure is K_2NiF_4-type with space group of I4/mmm.[6–15]

It is reported that Sr_2CoO_4 ceramics can only be prepared under high pressure, which may be due to the instability of intermediate spin state of Co^{4+} ions.[7–9,16] Meanwhile, sol–gel route as a very effective method has been successfully used to prepare Sr_2TiO_4 ceramics at relative low annealing temperatures from 850°C to 1050°C.[17,18] It is interesting to investigate whether the Co-doped Sr_2TiO_4 ceramics can be successfully prepared along with the variations in microstructures with Co doping. Moreover, the physical properties including transport and magnetic properties of $Sr_2Ti_{1-x}Co_xO_4$ have not yet been studied.

Herein, sol–gel is used to prepare $Sr_2Ti_{1-x}Co_xO_4$ ($0 \leq x \leq 0.3$) ceramics, and the Co doping effects on the microstructures as well as physical properties are investigated. The results show that crystallized phase can be obtained when $x \leq 0.3$. The magnetic moment is increased with Co doping and weak ferromagnetism at low temperatures is induced due to Co doping. The resistivity is decreased with Co doping and then increased with further Co doping.

2. Experimental

$Sr_2Ti_{1-x}Co_xO_4$ ($x = 0$, 0.1 and 0.3) ceramics were prepared by sol–gel method. Sr-acetate, Ti-*n*-butoxide and Co-acetate were dissolved into acetate acid and ethylene glycol, and the solution concentration was kept for 0.2 M for all three solutions. The solutions were dried at 200°C and 400°C in air, and the obtained powders were annealed at 1100°C in air with intermediate agitating. Finally, the powders were pressed into pellets and annealed at 1100°C in air for more than 48 h. It was observed that when the annealing temperature was lower than 1000°C, only phase-pure Sr_2TiO_4 can be obtained, whereas for the doped ceramics, 1100°C is the lowest annealing temperature to obtain phase-pure samples.

Powder X-ray diffraction (XRD) on a Philips X'pert Pro machine and transmission electron microscope (TEM, JEM-2010, JEOL Ltd., Japan) were used to check up the crystal phase and microstructures. Pellets were used to measure the electrical transport properties by the standard four-point probe technique. The magnetization measurements were performed on a Quantum Design superconducting quantum interface device for the three pellets.

3. Results and Discussion

Figure 1(a) shows the powder XRD results of all the three powders. It is observed that all the three samples are phase-pure of Sr_2TiO_4 phase without any detectable impurities (JCPDS No. 25-0915). As the Co content increases the XRD peak intensity is decreased since Sr_2TiO_4 can be easily prepared under ambient air, whereas Sr_2CoO_4 ceramics can be only prepared under high pressure.[8,9] With the Co doping content increasing, the crystal structure tends to be unstable, resulting in the decrease in the XRD intensity. As shown in the inset of Fig. 1(a), it is seen that

Mod. Phys. Lett. B 2017.31. Downloaded from www.worldscientific.com
by UNIVERSITY OF SCIENCE AND TECHNOLOGY OF CHINA on 06/06/18. For personal use only.

Mod. Phys. Lett. B 2017.31. Downloaded from www.worldscientific.com
by UNIVERSITY OF SCIENCE AND TECHNOLOGY OF CHINA on 06/06/18. For personal use only.

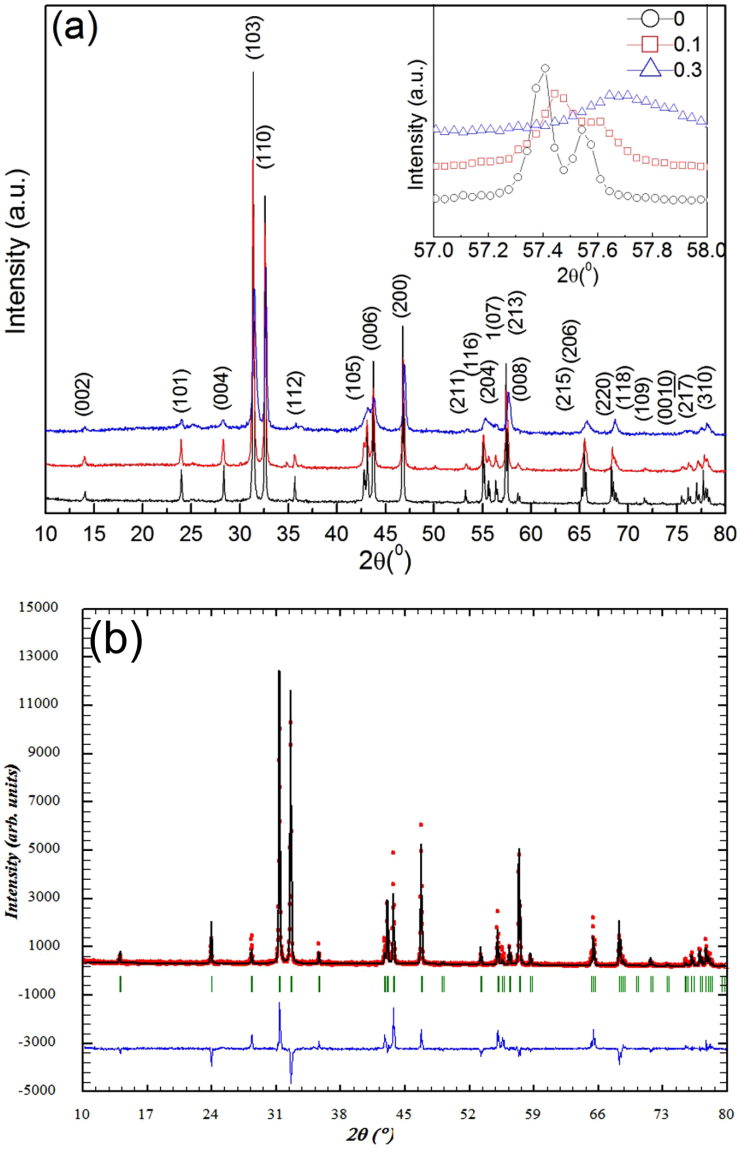

Fig. 1. (Color online) (a) XRD results of $Sr_2Ti_{1-x}Co_xO_4$ ($x = 0$, 0.1 and 0.3) ceramics and the inset shows the enlarged results and (b) Rietveld fitting result of the Sr_2TiO_4.

with the increase in Co content, the diffraction peak shifts to higher diffraction angle, suggesting the decrease in lattice constant. To give the variation of lattice constant with Co doping, Rietveld fittings are carried out for the three samples. Figure 1(b) shows the typical Rietveld fitting result of the Sr_2TiO_4 from which it is seen that the crystal structure is tetragonal and the lattice constants are $a = b = 3.884$ Å and $c = 12.590$ Å. The lattice constants obtained from Rietveld

Mod. Phys. Lett. B 2017.31. Downloaded from www.worldscientific.com
by UNIVERSITY OF SCIENCE AND TECHNOLOGY OF CHINA on 06/06/18. For personal use only.

fittings are $a = b = 3.873$ Å and $c = 12.570$ Å and $a = b = 3.863$ Å and $c = 12.397$ Å for the $Sr_2Ti_{0.9}Co_{0.1}O_4$ and $Sr_2Ti_{0.7}Co_{0.3}O_4$, respectively. The decrease in lattice constant with Co doping can be attributed to the smaller ionic radius of Co^{4+} as compared with that of Ti^{4+}. The average crystallite size is larger than 100 nm for the Sr_2TiO_4. On the other hand, with Co doping, the crystallite size is decreased and it is determined by Scherrer formula as 70 nm and 50 nm for the $Sr_2Ti_{0.9}Co_{0.1}O_4$ and the $Sr_2Ti_{0.7}Co_{0.3}O_4$, respectively, which is similar to the previous report about Sr_2TiO_4 ceramics prepared by sol–gel with the grain size of 50–60 nm under 1000°C annealing temperature.[18]

To further investigate the microstructures, TEM observations are carried out and the results are shown in Fig 2. Figure 2(a) shows the typical TEM result of

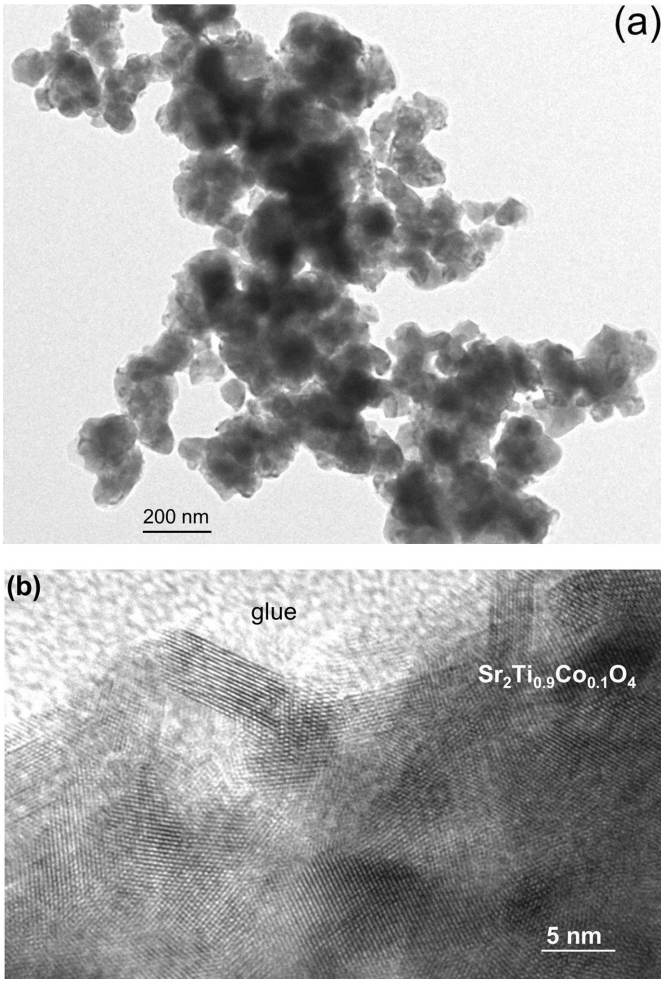

Fig. 2. TEM (a) HRTEM and (b) results of the prepared $Sr_2Ti_{0.9}Co_{0.1}O_4$ ceramics.

Mod. Phys. Lett. B 2017.31. Downloaded from www.worldscientific.com
by UNIVERSITY OF SCIENCE AND TECHNOLOGY OF CHINA on 06/06/18. For personal use only.

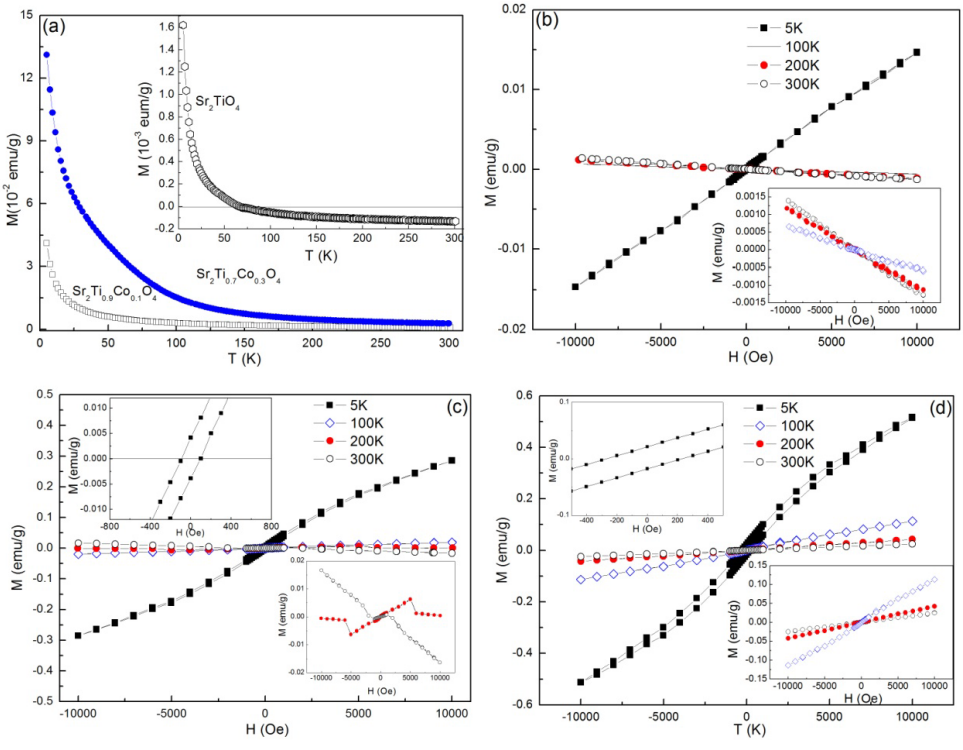

Fig. 3. (Color online) (a) ZFC M–T results of the Co-doped samples and the inset shows the ZFC M–T result of undoped sample and (b)–(d) M–H results of the Sr_2TiO_4, $Sr_2Ti_{0.9}Co_{0.1}O_4$ and $Sr_2Ti_{0.7}Co_{0.3}O_4$, respectively. The corresponding insets show the detailed M–H results.

the prepared $Sr_2Ti_{0.9}Co_{0.1}O_4$. It is seen that the average grain size is about 70–80 nm, which is similar to the result from XRD result. As shown in Fig. 2(b) of the high resolution TEM (HRTEM) result of the $Sr_2Ti_{0.9}Co_{0.1}O_4$, clear lattice strips are observed and there is no amorphous phase, suggesting the crystallized characteristics of the prepared $Sr_2Ti_{0.9}Co_{0.1}O_4$ceramics.

Temperature-dependent magnetization M–T of the zero-field-cooling (ZFC) model for all the three samples are measured with an applied magnetic field of 1000 Oe parallel to the sample surface, and the results are shown in Fig. 3(a). As shown in Fig. 3(a), it is seen that all the M–T curves behave like paramagnetic behaviors without any transitions, and the magnetic moment is sharply enhanced at low temperatures. As for the Sr_2TiO_4 as shown in the inset of Fig. 3(a), it is seen that the magnetic moment is negative at temperature higher than 72 K, which is attributed to the diamagnetism from the empty orbitals of the Ti^{4+} ions.[19,20] With Co doping, the diamagnetism at high temperatures is disappeared as for the $Sr_2Ti_{0.9}Co_{0.1}O_4$ and the $Sr_2Ti_{0.7}Co_{0.3}O_4$ due to the dilution of Ti^{4+} ions. Moreover, the magnetic moment is gradually enhanced with Co doping due to the partially occupied d orbitals of Co^{4+} ions. Figures 3(b)–3(d) show the magnetic hysteresis

Mod. Phys. Lett. B 2017.31. Downloaded from www.worldscientific.com
by UNIVERSITY OF SCIENCE AND TECHNOLOGY OF CHINA on 06/06/18. For personal use only.

loops at different temperatures for the three samples. From Fig. 3(b), it is seen that at high temperature, the Sr_2TiO_4 is diamagnetic, which is same as the M–T result due to the empty orbitals of the Ti^{4+} ions.[19,20] At 5 K, the magnetic moment is positive and increases linearly with the applied magnetic field, suggesting the paramagnetic property at low temperatures. With Co doping, the magnetic moment is enhanced obviously. At 5 K, the magnetic moment at an applied magnetic field of 1 T is enhanced from 0.015 emu/g for the Sr_2TiO_4 to 0.285 emu/g for the $Sr_2Ti_{0.9}Co_{0.1}O_4$ and 0.516 emu/g for the $Sr_2Ti_{0.7}Co_{0.3}O_4$. As shown in the bottom inset of Fig. 3(c) for the prepared $Sr_2Ti_{0.9}Co_{0.1}O_4$, at high temperatures, it is seen that a crossover in M–H loops from a paramagnetic-like to a diamagnetic-like behavior is observed with applied magnetic field increasing due to the enhanced diamagnetic effect from the empty orbitals of the Ti^{4+} ions with magnetic field increasing. Additionally, with temperature decreasing the crossover field is increased from 1000 Oe at 300 K to 5000 Oe at 200 K. With the temperature further decreasing to 100 K, the M–H loop is paramagnetic-like without any crossover. Moreover, at 5 K, the M–H loop shows ferromagnetic-like behavior and the coercivity is 100 Oe as shown in the upper inset of Fig. 3(c), which can be attributed to the superexchange effect from Co–O–Co as the ferromagnetism in Sr_2CoO_4.[6–9] As shown in Fig. 3(d) for the derived $Sr_2Ti_{0.7}Co_{0.3}O_4$, at high temperatures, the M–H loops show paramagnetic-like behaviors without the appearance of diamagnetic signals. Moreover, at 5 K, ferromagnetism is observed with the enhanced magnetic moment and the coercivity is enhanced to 230 Oe. The enhanced ferromagnetism can be attributed to the increased Co–O–Co superexchange with Co content ncreasing.

Figure 4(a) shows the temperature-dependent resistivity ρ–T of the $Sr_2Ti_{0.9}Co_{0.1}O_4$ and $Sr_2Ti_{0.7}Co_{0.3}O_4$ ceramics. It should be pointed out here that the resistivity of Sr_2TiO_4 is very large and cannot be measured by the four-probe method. The two samples behave like semiconductors with $d\rho/dT < 0$. Moreover, the resistivity of the $Sr_2Ti_{0.7}Co_{0.3}O_4$ within the measured temperature is higher than that of the $Sr_2Ti_{0.9}Co_{0.1}O_4$ ceramics. The resistivity at 300 K is 0.21×10^7 Ω cm and 0.51×10^7 Ω cm for the $Sr_2Ti_{0.9}Co_{0.1}O_4$ and $Sr_2Ti_{0.7}Co_{0.3}O_4$, respectively. Since Sr_2CoO_4 is metallic-like, it is expected that the resistivity should be decreased with the increasing Co doping content, which is different with our experimental results. On the other hand, the grain size is obviously decreased with the increase in Co doping content. The decreased grain size will lead to the enhanced resistivity due to the grain boundary effects.[21]

To investigate the electrical transport mechanisms, the ρ–T results are fitting and the results are shown in Fig. 4(b). It is found that the ρ–T results within the measured temperature range can be only well fitted by the Mott variable range hopping (VRH) model $\rho = \rho_0 \exp(T_0/T)^{1/4}$, where ρ_0 is a resistivity parameter and T_0 is a characteristic temperature (defined as Mott VRH temperature).[1] Additionally, the $(T_0)^{1/4}$ is increased from 73.5 $K^{1/4}$ for the $Sr_2Ti_{0.9}Co_{0.1}O_4$ to 74.4 $K^{1/4}$ for the $Sr_2Ti_{0.7}Co_{0.3}O_4$, suggesting the decreased electronic density of states at the Fermi

Mod. Phys. Lett. B 2017.31. Downloaded from www.worldscientific.com
by UNIVERSITY OF SCIENCE AND TECHNOLOGY OF CHINA on 06/06/18. For personal use only.

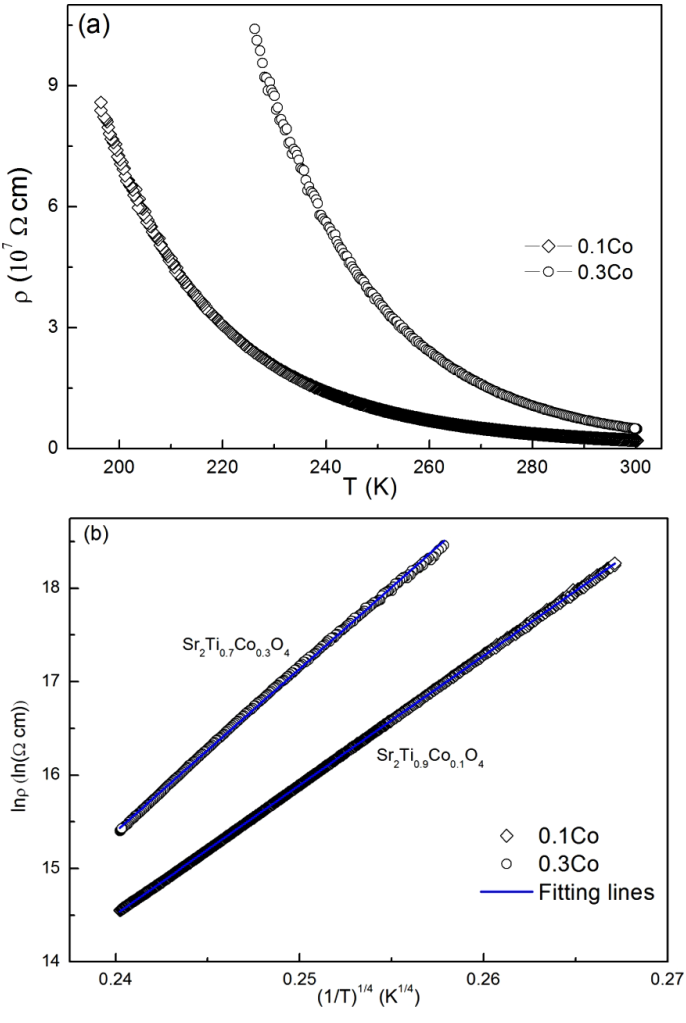

Fig. 4. (a) Temperature-dependent resistivity of $Sr_2Ti_{0.9}Co_{0.1}O_4$ and $Sr_2Ti_{0.7}Co_{0.3}O_4$ and (b) the Mott VRH fitting results of $Sr_2Ti_{0.9}Co_{0.1}O_4$ and $Sr_2Ti_{0.7}Co_{0.3}O_4$.

level and/or the localization length.[22] The good fittings by the Mott VRH model for the samples suggest that disorders play a very important role in the determination of the electrical transport properties, which can be attributed to the dilution of Ti sites by Co ions as well as the decreased grain size with Co doping.

4. Conclusion

$Sr_2Ti_{1-x}Co_xO_4$ ($0 \leq x \leq 0.3$) ceramics were prepared by sol–gel processing. The XRD results show that the prepared samples are phase-pure with tetragonal crystal structure. With Co doping, the XRD diffraction peak density is decreased and the grain size is also decreased. Magnetic property measurements show that the

magnetic moment is largely enhanced with Co doping, and ferromagnetism is observed for the Co-doped ceramics. The electrical transport properties of the Co-doped ceramics show semiconductor-like behaviors and the temperature-dependent resistivity can be well fitted by Mott VRH model. The resistivity of $Sr_2Ti_{0.9}Co_{0.1}O_4$ is lower than that of $Sr_2Ti_{0.7}Co_{0.3}O_4$ due to the decreased grain size. The results will provide an effective route to synthesize $Sr_2Ti_{1-x}Co_xO_4$ ceramics as well as to investigate the physical properties.

Mod. Phys. Lett. B 2017.31. Downloaded from www.worldscientific.com
by UNIVERSITY OF SCIENCE AND TECHNOLOGY OF CHINA on 06/06/18. For personal use only.

Acknowledgments

This work was supported by the National Natural Scientific Foundation of China under Nos. 11104001 and 21271007.

References

1. M. Imada, A. Fujimori and Y. Tokura, *Rev. Mod. Phys.* **70** (1998) 1039.
2. J. M. Tranquada, J. D. Axe, N. Ichikawa, Y. Nakamura, S. Uchida and B. Nachumi, *Phys. Rev. B* **54** (1996) 7489.
3. Y. Murakami, H. Kawada, H. Kawata, M. Tanaka, T. Arima, Y. Moritomo and Y. Tokura, *Phys. Rev. Lett.* **80** (1998) 1932.
4. F. Lichtenberg, A. Herrnberger and K. Wiedenmann, *Prog. Solid State Chem.* **36** (2008) 253.
5. W. Weng, Y. Kawazoe, X. Wan and J. Dong, *Phys. Rev. B* **74** (2006) 205112.
6. J. Matsuno, Y. Okimoto, Z. Fang, X. Z. Yu, Y. Matsui, N. Nagaosa, M. Kawasaki and Y. Tokura, *Phys. Rev. Lett.* **93** (2004) 167202.
7. X. L. Wang, E. Takayama-Muromachi, S. X. Dou and Z. X. Cheng, *Appl. Phys. Lett.* **91** (2007) 062501.
8. X. L. Wang, H. Sakurai and E. Takayama-Muromachi, *Phys. Rev. B* **72** (2005) 064401.
9. X. L. Wang and E. Takayama-Muromachi, *Appl. Phys. Lett.* **91** (2007) 062501.
10. J. Matsuno, Y. Okimoto, Z. Fang, X. Z. Yu, Y. Matsui, N. Nagaosa, H. Kumigashira, M. Oshima, M. Kawasaki and Y. Tokura, *Thin Solid Films* **486** (2005) 113.
11. K. W. Lee and W. E. Pickett, *Phys. Rev. B* **73** (2006) 174428.
12. S. K. Pandey, *Phys. Rev. B* **81** (2010) 035114.
13. P. K. Pandey, R. J. Choudhary and D. M. Phase, *Appl. Phys. Lett.* **103** (2013) 132413.
14. P. K. Pandey, R. J. Choudhary and D. M. Phase, *Appl. Phys. Lett.* **104** (2014) 182409.
15. H. Wu, *Phys. Rev. B* **86** (2012) 075120.
16. J. Wang, W. Zheng and Y. Xing, *Phys. Rev. B* **62** (2000) 14140.
17. N. Zhou, G. Chen, H. Z. Xian and H. J. Zhang, *Mater. Res. Bull.* **43** (2008) 2554.
18. T. Ahmad and A. K. Ganguli, *J. Am. Ceram. Soc.* **89** (2006) 1326.
19. M. Muralidharan, V. Anbarasu, A. E. Perumal and K. Sivakumar, *J. Mater. Sci. Mater. Electron.* **26** (2015) 6352.
20. T. E. Phan, P. D. Thang, T. A. Ho, T. V. Manh, T. D. Thanh, V. D. Lam, N. T. Dang and S. C. Yu, *J. Appl. Phys.* **117** (2015) 17D904.
21. P. Kameli, H. Salamati and A. Aezami, *J. Alloys Compd.* **450** (2008) 7.
22. L. Zhang, G. Liu, Z. Tang, Y. Deng, Y. Li, J. Yu and X. Zhu, *Physica B: Condens. Matter* **451** (2014) 73.